than 0.15. The final Fourier difference map showed no peak greater than 0.59 e/Å^3.

Acknowledgment. This work has been supported by grants from Research Corp. and from the donors of the Petroleum Research Fund, administered by the American Chemical Society. Acknowledgment is also made to the NSF EPSCoR program (Grant No. RII-8610680) for partial support of this research. We thank Dr. Carron for obtaining the Raman spectrum of complex 2 and Drs. Buttry and Borjas for assistance with the electrochemical experiments.

Note Added in Proof. Two structural reports of fluorophosphine Mo(0) complexes with very short Mo(0)–P bond distances comparable to those detailed in this paper have been brought to our attention.[53,54]

Supplementary Material Available: Tables of complete data collection parameters, atomic coordinates for **6**, bond distances, bond angles, anisotropic thermal parameters, and hydrogen atom coordinates and isotropic thermal parameters (19 pages); listings of calculated and observed structure factors (38 pages). Ordering information is given on any current masthead page.

(53) Mo–P = 2.336–2.411 Å: Newton, M. G.; King, R. B.; Lee, T.-W.; Norskov-Lauritzen, L.; Kumar, V. *J. Chem. Soc., Chem. Commun.* **1982**, 201.

(54) Mo–P = 2.331–2.350 Å: Brown, G. M.; Finholt, J. E.; King, R. B.; Lee, T. W. *J. Am. Chem. Soc.* **1981**, *103*, 5249.

Models for Multicenter Catalysts. 4.[1-3] Reactions of Binuclear Hydrides with Alkynes and the Structure of $[Ir_2(H)_2Cl(CH_3O_2CC{=}C(H)CO_2CH_3)_2(CO)_2(Ph_2PCH_2PPh_2)_2]$-$[BF_4]$·3THF, a Model Hydrogenation Intermediate Containing Mutually Adjacent Alkenyl and Hydrido Ligands

Brian A. Vaartstra and Martin Cowie*

Department of Chemistry, The University of Alberta, Edmonton, Alberta, Canada T6G 2G2

Received October 26, 1989

The reaction of $[Ir_2(H)_2(CO)_2(\mu\text{-}Cl)(DPM)_2][BF_4]$ (1) with 2 equiv of dimethyl acetylenedicarboxylate (DMA) in THF or acetone yields $[Ir_2(CH_3O_2CC{=}C(H)CO_2CH_3)_2(CO)_2(\mu\text{-}Cl)(DPM)_2][BF_4]$. This cationic species is the result of alkyne insertion into both of the Ir–H bonds of compound 1. Further reaction of this species with dihydrogen yields $[Ir_2(H)_2Cl(CH_3O_2CC{=}C(H)CO_2CH_3)_2(CO)_2(DPM)_2][BF_4]$ (DPM = $Ph_2PCH_2PPh_2$), which is a stable complex containing mutually adjacent alkenyl and hydrido ligands. This compound crystallizes in the space group $P2_1/c$ with a = 18.675 (5) Å, b = 15.775 (3) Å, c = 26.371 (4) Å, β = 96.38 (2)°, and Z = 4. The structure has refined to R = 0.054 and R_w = 0.062 on the basis of 5775 unique observations and 590 parameters varied. Although the hydride ligands were not directly located in the X-ray study, their positions can be inferred from the positions of the heavy atoms and from the NMR studies. One is located in a terminal site on one Ir adjacent to an alkenyl group, while the other is bridging the two metals, resulting in an Ir–Ir separation of 3.2895 (7) Å. A mechanism is proposed for one pathway by which alkynes may be hydrogenated by binuclear species such as 1. It is proposed that hydrogenation occurs at each individual metal center in turn but that the coordinative unsaturation required at different stages occurs by movement of the chloride ligand back and forth from one metal to the other. The reactions of 1 with 2-butyne and ethylene yield 2-butenes and ethane, respectively, in the absence of H_2 and suggest an alternate intermolecular mechanism for hydrogenation. The reaction of alkynes with the mixed-metal species, $[RhIr(H)_2(CO)_2(\mu\text{-}Cl)(DPM)_2]^+$, does not appear to result in insertion but rather displaces H_2 from the complex, yielding alkyne-bridged species.

Introduction

Preliminary studies done within this research group[1-5] have attempted to delineate the sites of attack, accessible bonding modes, and ligand mobilities involved in reactions of dihydrogen and unsaturated substrates with binuclear DPM-bridged complexes (DPM = $Ph_2PCH_2PPh_2$). One of the primary goals of such studies was to gain information relevant to alkyne hydrogenation catalysis in the presence of two or more adjacent metals. It has been shown that alkyne hydrogenation is catalyzed by the binuclear complexes $[Rh_2(CO)_2(\mu\text{-}Cl)(DPM)_2][BPh_4]$,[6] $[Rh_2(H)_2(CO)_2(DPM)_2]$,[7,8] and $[Rh_2Cl_2(\mu\text{-}CO)(DPM)_2]$,[9] although information about possible intermediates was lacking. Of particular interest were suggestions[1,10,11] that the two ad-

(1) Sutherland, B. R.; Cowie, M. *Organometallics* **1985**, *4*, 1801.
(2) Sutherland, B. R.; Cowie, M. *Organometallics* **1984**, *3*, 1869.
(3) Vaartstra, B. A.; O'Brien, K. N.; Eisenberg, R.; Cowie, M. *Inorg. Chem.* **1988**, *27*, 3668.
(4) Vaartstra, B. A.; Cowie, M. *Inorg. Chem.* **1989**, *28*, 3138.
(5) Vaartstra, B. A.; Cowie, M. *Organometallics* **1989**, *8*, 2388.
(6) Sanger, A. R. *Prepr.—Can. Symp. Catal.* **1979**, *6*, 37.
(7) Kubiak, C. P.; Woodcock, C.; Eisenberg, R. *Inorg. Chem.* **1982**, *21*, 2119.
(8) Woodcock, C.; Eisenberg, R. *Inorg. Chem.* **1984**, *23*, 4207.
(9) Cowie, M.; Southern, T. G. *Inorg. Chem.* **1982**, *21*, 246.
(10) Kubiak, C. P.; Woodcock, C.; Eisenberg, R. *J. Am. Chem. Soc.* **1977**, *99*, 6129.

0276-7333/90/2309-1594$02.50/0

jacent metal centers might be involved cooperatively at some stage of the catalytic cycle in such systems.

Substitution of iridium for one or both metals in the above complexes has already proven to be an advantage over the dirhodium systems, yielding isolable and characterizable hydrides upon reaction with H_2.[1,3,4,12,13] These hydride complexes therefore represent potential models of intermediates proposed to be involved in catalytic hydrogenation by binuclear complexes. It has also been shown[1,3-5] that the mobility of the anionic bridging group in binuclear diiridium or rhodium-iridium complexes can be instrumental in allowing both hydrides and coordinated alkynes to migrate within the framework of the two-metal systems and in generating coordinative unsaturation at the metals. These results and a preliminary study[1] of the reactivity of one of these hydrides, $[Ir_2(H)_2(CO)_2(\mu\text{-}Cl)(DPM)_2][BF_4]$ (1), with dimethyl acetylenedicarboxylate, which resulted in insertion of alkyne moieties into both Ir-H bonds, suggested that further study was warranted.

In this paper, subsequent steps toward successfully modeling catalytic hydrogenation at adjacent metal centers is investigated by further study into the reaction of 1 and the mixed-metal analogue, $[RhIr(H)_2(CO)_2(\mu\text{-}Cl)(DPM)_2][BF_4]$, with unsaturated substrates.

Experimental Section

All solvents were appropriately dried and distilled prior to use and were stored under dinitrogen. Reactions were carried out under standard Schlenk conditions using dinitrogen that had been passed through columns containing Ridox and 4A molecular sieves in order to remove traces of oxygen and water, respectively. Hydrated iridium trichloride was obtained from Johnson-Matthey, $RhCl_3 \cdot 3H_2O$ from Engelhard, and bis(diphenylphosphino)methane from Strem Chemicals. Dihydrogen and ethylene were obtained from Linde and used as received. Dimethyl acetylenedicarboxylate (DMA), 2-butyne, and phenylacetylene were purchased from Aldrich Chemical Co. Tetrafluoroethylene was purchased from PCR incorporated. The compounds $[Ir_2(H)_2(CO)_2(\mu\text{-}Cl)(DPM)_2[BF_4]$[1] and $[RhIr(H)_2(CO)_2(\mu\text{-}Cl)(DPM)_2][X]$ (X = Cl, BF_4)[4] were prepared according to the previously reported procedures. The hydrogenation of 2-butyne was followed by sampling the gases above reaction mixtures with a gastight syringe (Hamilton) and analyzing them by gas chromatography on a Perkin-Elmer 8500 gas chromatograph using a Chromosorb W-AW column at 25 °C. Retention times and approximate quantities of product gases were determined from calibration plots using the pure gases. Attempted catalytic runs for the hydrogenation of ethylene were performed at 22 °C using a hydrogen-uptake apparatus (gas buret) to monitor the progress of the reaction. Mass spectroscopy experiments were carried out on a Kratos MS50 spectrometer by the service within the department. The $^{31}P\{^1H\}$, ^1H, and $^1H\{^{31}P\}$ NMR spectra were recorded on a Bruker WH-400 spectrometer. Infrared spectra were recorded on a Nicolet 7199 Fourier transform IR spectrometer either as solids in Nujol mulls on KBr plates or as solutions in KCl cells with 0.5-mm window path lengths. Elemental analyses were performed by the microanalytical service within the department. Conductivity measurements were made on approximately 10^{-3} M solutions using a Yellow Springs Instrument Co. Model 31 conductivity bridge.

Preparation of Compounds. (a) $[Ir_2(CH_3O_2CC{=}C(H)CO_2CH_3)_2(CO)_2(\mu\text{-}Cl)(DPM)_2][BF_4]$ (2). To a suspension of $[Ir_2(H)_2(CO)_2(\mu\text{-}Cl)(DPM)_2][BF_4]$ (1, 200.0 mg, 0.150 mmol) in 15 mL of THF (or acetone) was added an excess of dimethyl acetylenedicarboxylate (DMA, 50.0 μL, 0.407 mmol). Within minutes the solution changed color from yellow to orange-yellow. After 1 h the solution was concentrated to a volume of 5 mL under dinitrogen from which a bright yellow microcrystalline solid was precipitated by the addition of 40 mL of diethyl ether. The solid was collected, washed with two 10-mL portions of diethyl ether, and dried in vacuo, giving typical isolated yields of 80–85%. Anal. Calcd for $Ir_2ClP_4F_4O_{10}C_{64}BH_{58}$: C, 47.52; H, 3.61; Cl, 2.19. Found: C, 47.32; H, 3.55; Cl, 2.77. $^{31}P\{^1H\}$ NMR (THF) δ −13.62 (s); ^1H NMR δ 5.32 (m, 2 H), 4.46 (m, 2 H), 3.52 (s, 2 H), 3.39 (s, 6 H), 3.21 (s, 6 H); IR (cm^{-1}, Nujol) 2028 (vs), 2013 (vs) (ν(CO)), 1713 (vs) (ν(C=O) of CO_2CH_3), 1573 (ν(C=C)).[14]

(b) $[Ir_2(H)_2Cl(CH_3O_2CC{=}C(H)CO_2CH_3)_2(CO)_2(DPM)_2][BF_4]$ (3). The dinitrogen atmosphere over a solution of 2 (100.0 mg, 0.062 mmol) in 10 mL of THF (or acetone) was displaced by an atmosphere of dihydrogen. Immediately the solution changed color from orange-yellow to pale yellow. The solution was stirred for an additional 30 min under H_2 and then concentrated to 5 mL with rapid H_2 flow. Compound 3 was precipitated by the addition of 25 mL of diethyl ether, collected, and washed with two additional 5-mL volumes of diethyl ether. The resulting colorless microcrystalline solid was dried with a dihydrogen purge, giving 3 in 90% yield. Anal. Calcd for $Ir_2ClP_4F_4O_{10}C_{64}BH_{60}$: C, 47.46; H, 3.73; Cl, 2.19. Found: C, 47.68; H, 3.68; Cl, 2.10. $^{31}P\{^1H\}$ NMR (acetone-d_6, −40 °C) δ −7.90 (m), −12.77 (m); ^1H NMR δ 6.44 (m, 2 H), 5.24 (m, 2 H), 4.32 (s, 1 H), 3.62 (s, 1 H), 3.52 (s, 3 H), 3.46 (s, 3 H), 3.33 (s, 3 H), 3.10 (s, 3 H), −8.76 (t, 1 H, $^2J_{P-H}$ = 18.4 Hz), −19.37 (br, 1 H); IR (cm^{-1}, CH_2Cl_2) 2135 (w) (ν(Ir-H)); 2051 (vs), 2016 (med) (ν(CO)), 1709 (vs) (ν(C=O) of CO_2CH_3), 1588 (ν(C=C)).[14]

Hydrogenation Reactions. (a) Ethylene. A solution of $[Ir_2(H)_2Cl(CO)_2(DPM)_2][BF_4]$ and $[Ir_2(D)_2Cl(CO)_2(DPM)_2][BF_4]$ (20 mg of each in 2 mL of CH_2Cl_2) was evacuated, and then the flask was charged with 1 atm of ethylene at room temperature, causing the solution to turn orange within 15 min. After 2 h the gases above the solution were sampled by syringe and analyzed by using a Kratos MS50 mass spectrometer.

(b) 2-Butyne. A solution of 1 (50 mg in 4 mL of CH_2Cl_2 or THF) was reacted with 2-butyne, causing an immediate color change from yellow to orange. Over 20 min the color changed to red-orange, and $^{31}P\{^1H\}$ and ^1H NMR and IR spectra identified $[Ir_2(CO)_2(\mu\text{-}Cl)(DPM)_2][BF_4]$[15] as the only iridium-phosphine product. Analysis of the gases above the solution by gas chromatography (Perkin-Elmer Model 8500) revealed nearly equal concentrations of *cis*- and *trans*-2-butene, together with residual 2-butyne and a small amount (ca. 10% based on moles of complex) of 1-butene.

X-ray Data Collection. Crystals of compound 3 suitable for X-ray diffraction studies were obtained by slow diffusion of diethyl ether into a saturated THF solution of the compound. The crystals proved susceptible to loss of both solvent of crystallization and H_2, so one was selected and wedged into a capillary tube containing H_2 and solvent vapor, which was then flame sealed. Data were collected on an Enraf-Nonius CAD4 diffractometer at 22 °C using graphite-monochromated Mo Kα radiation. Unit cell parameters were obtained from a least-squares refinement of the setting angles of 25 reflections in the range 21.8° $\leq 2\theta \leq$ 25.2°. A monoclinic crystal system was established by the usual peak search and reflection indexing programs and systematic absences ($h0l$, l = odd; $0k0$, k = odd) in the data were consistent with the space group $P2_1/c$.

Intensity data were collected on the CAD4 diffractometer as described previously.[4] The intensities of three standard reflections, measured every hour of exposure time, showed a mean decrease of 9.2% and a correction was applied to the data assuming linear decay. The data were processed in the usual manner on a Digital PDP 11/23 PLUS computer.[16] See Table I for pertinent crystal data and details of intensity collection.

Structure Solution and Refinement. The structure was solved by using Patterson techniques to locate the metals and by successive least-squares and difference Fourier calculations to obtain the other atom positions. Hydrogen atoms associated with the DPM ligands and carboxylate methyl groups were located but were assigned to idealized positions as described previously.[4]

(11) Poilblanc, R. *Inorg. Chim. Acta* **1982**, *62*, 75.
(12) McDonald, R.; Sutherland, B. R.; Cowie, M. *Inorg. Chem.* **1987**, *26*, 3333.
(13) McDonald, R.; Cowie, M. *Inorg. Chem.*, in press.

(14) Abbreviations: s, singlet, m, multiplet; br, broad; t, triplet; vs, very strong; w, weak; med, medium.

(15) Sutherland, B. R.; Cowie, M. *Inorg. Chem.* **1984**, *23*, 2324.

(16) Programs used were those of the Enraf-Nonius Structure Determination Package by B. A. Frenz, in addition to local programs by R. G. Ball.

Table I. Summary of Crystal Data and Details of Intensity Collection

compd	$[Ir_2(H)_2Cl(CH_3O_2CC{=}C(H)CO_2CH_3)_2(CO)_2(DPM)_2][BF_4]\cdot 3THF$
formula	$Ir_2ClP_4F_4O_{13}C_{76}BH_{84}$
fw	1836.09
cryst shape	irregular plate
cryst size, mm	0.58 × 0.35 × 0.06
space group	$P2_1/c$ (No. 14)
cell params	
a, Å	18.675 (5)
b, Å	15.775 (3)
c, Å	26.371 (4)
β, deg	96.38 (2)
V, Å^3	7720.6
Z	4
ρ(calcd), g/cm^3	1.517
temp, °C	22
radiation (λ, Å)	graphite monochromated Mo Kα (0.71069)
receiving aperture, mm	3.00 + (tan θ) wide × 4.00 high, 173 from crystal
takeoff angle, deg	3.00
scan speed, deg/min	variable between 6.67 and 0.95
scan width, deg	0.50 + (0.347 tan θ) in θ
2θ limits, deg	$1.0 \le 2\theta \le 48.0$
no. of unique data collcd	12079 ($h,k,\pm l$)
no. of unique data used ($F_o^2 \ge 3\sigma(F_o^2)$)	5775
linear absorption coeff μ, cm^{-1}	36.10
range of transm factors	0.891-1.362
final no. of params refined	590
error in observation of unit weight	1.752
R^a	0.054
$R_w^{\ b}$	0.062

$^a R = \sum||F_o| - |F_c||/\sum|F_o|$. $^b R_w = [\sum w(|F_o| - |F_c|)^2/\sum wF_o^2]^{1/2}$.

Two of the solvent molecules were reasonably well behaved, but electron density associated with them was somewhat smeared out. The third sppeared slightly disordered such that its oxygen and carbon atoms could not be differentiated; all atoms in this ring were therefore refined as carbons. The hydrogen atoms of the solvent molecules were not included in the refinement owing to the high thermal parameters associated with the carbon and oxygen atoms.

Refinement in the space group $P2_1/c$ converged at $R = 0.054$ and $R_w = 0.062$. The final positional and isotropic thermal parameters for all non-hydrogen atoms are given in Table II. The 10 highest peaks in the final difference Fourier map (0.993–0.623 e/Å^3) were in the vicinities of the metals and the THF solvent molecules.

Results and Discussion

(a) Description of Structure. Compound **3** crystallizes in the space group $P2_1/c$ with one complex cation, the BF_4^- anion, and three THF solvent molecules in the asymmetric unit. The BF_4^- anion is well-behaved and displays the expected tetrahedral geometry. Although the solvent molecules were found to have high thermal parameters, their geometries are as expected and there are no unusual contacts between the solvent molecules, the BF_4^- anion, or the complex cation. A perspective view of the complex cation is shown in Figure 1, and a view containing only the metals and equatorial ligands is shown in Figure 2. Selected bond distances and angles are given in Tables III and IV, respectively.

The complex exhibits a geometry in which each metal has a distorted octahedral coordination with the hydrido ligands situated as shown in the figures. The major distortion from octahedral geometries at the metal centers is due to the DPM ligands. As was found in the complex obtained from Cl^- addition to **2**, $[Ir_2Cl_2(CH_3O_2CC{=}C(H)CO_2CH_3)_2(CO)_2(DPM)_2]$,[1] both DPM ligands in complex **3** are tilted away from the side of the molecule containing the carbonyl ligands and the carboxylate groups which are nearest the metals. The resulting angles at Ir(1) (P(1)–Ir(1)–C(1) = 96.3 (4)° and P(3)–Ir(1)–C(1) = 97.1 (4)°) are very similar to those found in the dichloro complex. At Ir(2), however, the angles are slightly greater (P(2)–Ir(2)–C(2) = 104.6 (4)° and P(4)–Ir(2)–C(2) = 99.2 (4)°), indicating less steric congestion opposite C(2). Although the Ir–P distances at Ir(2) (2.354 (3), 2.346 (3) Å) are similar to those found in the neutral dichloro complex, those at Ir(1) are slightly longer (2.399 (3), 2.388(3) Å) owing to the greater steric congestion caused by the larger chloro ligand on Ir(1). The congestion at this metal results in some rather close nonbonded contacts between phenyl hydrogens and the carbonyl oxygen atoms (O(1)–H(36) = 2.26 Å, O(2)–H(42) = 2.57 Å). These distances are rather short compared to the sums of the van der Waals radii involved.[17]

Although the hydrido ligands were not located crystallographically, their approximate positions are assigned on the basis of ^1H NMR spectroscopic data (vide infra) and the positions of the other ligands in the structure. The position of the terminal hydride is obvious from the vacant coordination site opposite C(2), and the bridging hydride is suggested to be part of a nearly collinear Ir–H–Ir linkage. Such positions are consistent with the octahedral geometry of the complex, and furthermore the Ir–Ir separation of 3.2895 (7) Å is almost exactly what would be predicted based on sums of covalent radii for the Ir atoms and the

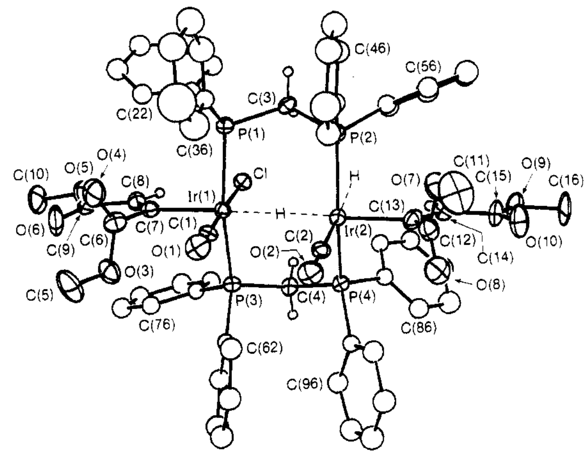

Figure 1. Perspective view of the $[Ir_2(H)_2Cl(CH_3O_2CC{=}C(H)CO_2CH_3)_2(CO)_2(DPM)_2]^+$ cation showing the numbering scheme. Thermal parameters are shown at the 20% level except for the methylene hydrogens, which are shown artificially small. The hydrido ligands, which were not located, are shown in their idealized positions.

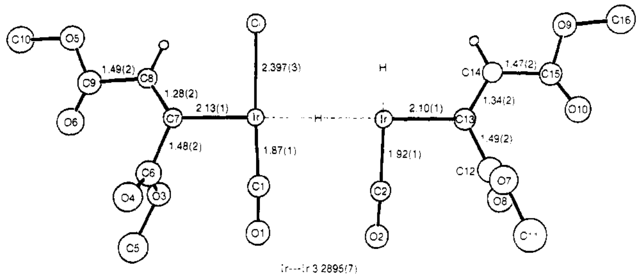

Figure 2. View of the approximate equatorial plane of the complex, including some relevant bond distances.

(17) Huheey, J. E. *Inorganic Chemistry*, 3rd ed.; Harper and Row: New York, 1983; pp 258–259 and references therein.

Table II. Positional Parameters and Isotropic Thermal Parameters[a]

atom	x	y	z	B, Å²	atom	x	y	z	B, Å²
Ir(1)	0.23047 (3)	0.09135 (4)	-0.07859 (2)	3.55 (1)	C(41)	0.2948 (8)	0.2094 (9)	-0.2451 (6)	4.4 (3)*
Ir(2)	0.26816 (3)	0.00253 (4)	-0.18532 (2)	3.71 (1)	C(42)	0.365 (1)	0.202 (1)	-0.2280 (7)	7.1 (5)*
Cl	0.1051 (2)	0.0596 (2)	-0.0989 (1)	4.27 (9)	C(43)	0.415 (1)	0.269 (1)	-0.2412 (8)	10.1 (6)*
P(1)	0.1980 (2)	0.2179 (3)	-0.1261 (2)	4.1 (1)	C(44)	0.386 (1)	0.337 (1)	-0.2692 (7)	7.8 (5)*
P(2)	0.2326 (2)	0.1296 (3)	-0.2277 (2)	4.2 (1)	C(45)	0.316 (1)	0.343 (1)	-0.2839 (7)	7.6 (5)*
P(3)	0.2351 (2)	-0.0479 (3)	-0.0429 (2)	3.69 (9)	C(46)	0.2689 (9)	0.278 (1)	-0.2719 (7)	6.5 (4)*
P(4)	0.2513 (2)	-0.1311 (3)	-0.1494 (2)	3.8 (1)	C(51)	0.1738 (8)	0.1064 (9)	-0.2864 (6)	4.5 (4)*
F(1)	0.9035 (5)	0.6415 (6)	0.2537 (4)	8.1 (3)	C(52)	0.1095 (9)	0.069 (1)	-0.2855 (6)	5.8 (4)*
F(2)	0.9032 (7)	0.5182 (7)	0.2081 (4)	10.9 (4)	C(53)	0.069 (1)	0.042 (1)	-0.3306 (7)	7.7 (5)*
F(3)	0.8483 (7)	0.5261 (7)	0.2803 (5)	12.0 (4)	C(54)	0.099 (1)	0.053 (1)	-0.3753 (7)	7.0 (5)*
F(4)	0.9703 (8)	0.5307 (8)	0.2822 (6)	13.7 (5)	C(55)	0.164 (1)	0.090 (1)	-0.3771 (7)	7.4 (5)*
O(1)	0.3862 (6)	0.1322 (7)	-0.0576 (5)	7.2 (3)	C(56)	0.2046 (9)	0.116 (1)	-0.3340 (6)	5.6 (4)*
O(2)	0.4290 (6)	0.0249 (7)	-0.1467 (5)	7.0 (3)	C(61)	0.3205 (7)	-0.0957 (8)	-0.0148 (5)	3.6 (3)*
O(3)	0.3162 (6)	0.1250 (7)	0.0491 (4)	7.1 (3)	C(62)	0.3861 (9)	-0.070 (1)	-0.0271 (6)	6.3 (4)*
O(4)	0.2928 (8)	0.2574 (8)	0.0190 (5)	9.7 (4)	C(63)	0.4497 (9)	-0.114 (1)	-0.0074 (7)	6.6 (5)*
O(5)	0.0734 (6)	0.1687 (8)	0.0719 (4)	7.5 (4)	C(64)	0.443 (1)	-0.182 (1)	0.0245 (7)	6.9 (5)*
O(6)	0.1879 (7)	0.1950 (9)	0.0935 (5)	9.7 (4)	C(65)	0.3776 (9)	-0.207 (1)	0.0359 (7)	7.1 (5)*
O(7)	0.3668 (7)	0.0314 (8)	-0.2969 (5)	8.7 (4)	C(66)	0.3144 (9)	-0.164 (1)	0.0157 (6)	5.6 (4)*
O(8)	0.4129 (6)	-0.0810 (9)	-0.2571 (5)	8.7 (4)	C(71)	0.1755 (7)	-0.0636 (9)	0.0063 (5)	3.8 (3)*
O(9)	0.1940 (6)	-0.1742 (7)	-0.3563 (4)	7.0 (3)	C(72)	0.1064 (8)	-0.098 (1)	-0.0038 (6)	5.0 (4)*
O(10)	0.3080 (6)	-0.1312 (9)	-0.3524 (4)	8.7 (4)	C(73)	0.0624 (9)	-0.102 (1)	0.0362 (7)	6.7 (4)*
O(11)[b]	0.439 (1)	0.468 (2)	0.055 (1)	23 (1)	C(74)	0.0876 (9)	-0.073 (1)	0.0835 (6)	5.9 (4)*
O(12)[b]	0.852 (1)	0.444 (2)	0.089 (1)	25 (1)	C(75)	0.1562 (9)	-0.040 (1)	0.0955 (7)	6.1 (4)*
C(1)	0.3286 (8)	0.1154 (9)	-0.0660 (5)	4.2 (4)	C(76)	0.1993 (8)	-0.036 (1)	0.0561 (6)	4.8 (4)*
C(2)	0.3685 (8)	0.0187 (9)	-0.1619 (6)	4.4 (4)	C(81)	0.1879 (8)	-0.1984 (9)	-0.1902 (6)	4.2 (3)*
C(3)	0.1698 (7)	0.1875 (9)	-0.1922 (6)	4.2 (4)	C(82)	0.1179 (8)	-0.1737 (9)	-0.2002 (6)	4.6 (4)*
C(4)	0.2026 (7)	-0.1231 (8)	-0.0926 (5)	3.7 (3)	C(83)	0.0678 (9)	-0.227 (1)	-0.2298 (6)	5.9 (4)*
C(5)	0.377 (1)	0.164 (2)	0.0804 (8)	11.2 (8)	C(84)	0.091 (1)	-0.300 (1)	-0.2480 (7)	7.1 (5)*
C(6)	0.2745 (9)	0.183 (1)	0.0216 (7)	6.3 (5)	C(85)	0.163 (1)	-0.325 (1)	-0.2388 (7)	7.9 (5)*
C(7)	0.2099 (8)	0.1442 (9)	-0.0074 (6)	4.1 (4)	C(86)	0.2124 (9)	-0.274 (1)	-0.2077 (6)	5.9 (4)*
C(8)	0.1493 (8)	0.140 (1)	0.0108 (6)	4.9 (4)	C(91)	0.3302 (7)	-0.1991 (9)	-0.1328 (5)	3.9 (3)*
C(9)	0.1417 (9)	0.173 (1)	0.0627 (6)	6.0 (5)	C(92)	0.3895 (9)	-0.190 (1)	-0.1550 (6)	6.0 (4)*
C(10)	0.063 (1)	0.192 (1)	0.1247 (7)	9.6 (6)	C(93)	0.449 (1)	-0.246 (1)	-0.1441 (7)	6.8 (5)*
C(11)	0.439 (1)	0.050 (2)	-0.311 (1)	13.2 (8)	C(94)	0.444 (1)	-0.308 (1)	-0.1115 (7)	7.3 (5)*
C(12)	0.3627 (9)	-0.036 (1)	-0.2682 (6)	6.3 (5)	C(95)	0.3860 (9)	-0.322 (1)	-0.0888 (7)	7.0 (5)*
C(13)	0.2885 (8)	-0.052 (1)	-0.2551 (6)	5.5 (4)	C(96)	0.3260 (9)	-0.265 (1)	-0.0968 (6)	5.8 (4)*
C(14)	0.2387 (8)	-0.094 (1)	-0.2860 (6)	5.2 (4)	C(100)[b]	0.418 (2)	0.561 (2)	0.054 (1)	18 (1)*
C(15)	0.2519 (9)	-0.134 (1)	-0.3344 (6)	5.9 (4)	C(101)[b]	0.342 (2)	0.543 (2)	0.027 (1)	23 (1)*
C(16)	0.203 (1)	-0.218 (1)	-0.4032 (7)	10.6 (7)	C(102)[b]	0.331 (2)	0.457 (3)	0.032 (2)	26 (2)*
C(21)	0.1188 (7)	0.2705 (9)	-0.1065 (5)	3.9 (3)*	C(103)[b]	0.402 (3)	0.426 (3)	0.015 (2)	33 (2)*
C(22)	0.1295 (8)	0.311 (1)	-0.0586 (6)	5.5 (4)*	C(104)[b]	0.897 (2)	0.423 (2)	0.041 (1)	20 (1)*
C(23)	0.067 (1)	0.351 (1)	-0.0414 (7)	6.7 (5)*	C(105)[b]	0.892 (1)	0.318 (2)	0.047 (1)	14.2 (9)*
C(24)	0.0043 (9)	0.350 (1)	-0.0699 (7)	6.7 (5)*	C(106)[b]	0.825 (1)	0.332 (2)	0.050 (1)	13.9 (9)*
C(25)	-0.004 (1)	0.311 (1)	-0.1149 (7)	7.4 (5)*	C(107)[b]	0.880 (2)	0.352 (2)	0.102 (2)	21 (1)*
C(26)	0.0531 (9)	0.270 (1)	-0.1342 (6)	6.0 (4)*	C(108)[b]	0.616 (2)	0.433 (2)	0.343 (1)	19 (1)*
C(31)	0.2602 (8)	0.3042 (9)	-0.1290 (6)	4.5 (4)*	C(109)[b]	0.572 (2)	0.352 (2)	0.317 (1)	17 (1)*
C(32)	0.237 (1)	0.376 (1)	-0.1514 (8)	8.6 (6)*	C(110)[b]	0.635 (2)	0.321 (2)	0.283 (1)	27 (1)*
C(33)	0.283 (1)	0.445 (1)	-0.1610 (8)	9.1 (6)*	C(111)[b]	0.674 (2)	0.418 (2)	0.311 (1)	22 (1)*
C(34)	0.350 (1)	0.444 (1)	-0.1397 (8)	9.4 (6)*	C(112)[b]	0.617 (3)	0.407 (3)	0.270 (2)	22 (2)*
C(35)	0.379 (2)	0.370 (2)	-0.117 (1)	17 (1)*	B	0.907 (1)	0.553 (2)	0.2566 (9)	7.7 (6)*
C(36)	0.328 (1)	0.300 (1)	-0.1138 (9)	10.8 (7)*					

[a] Estimated standard deviations in these and subsequent tables are given in parentheses and correspond to least significant digits. Atoms with asterisks were refined isotropically. Anisotropically refined atoms are given in the form of the isotropic equivalent displacement parameter defined as $^4/_3[a^2\beta(1,1) + b^2\beta(2,2) + c^2\beta(3,3) + ab(\cos\gamma)\beta(1,2) + ac(\cos\beta)\beta(1,3) + bc(\cos\alpha)\beta(2,3)]$. [b] The THF solvent molecules are labelled as follows: THF (1): O(11), C(100), C(101), C(102), C(103). THF(2): O(12), C(104), C(105), C(106), C(107). THF(3): C(108), C(109), C(110), C(111), C(112); see text regarding disorder of this molecule.

bridging hydrido ligand (3.27 Å).[17] It should be pointed out that for all cases of hydride-bridged metal complexes in which the hydrido ligand was located (either by X-ray or neutron diffraction), the M–H–M linkage is bent, with angles ranging from 85° to 159°.[18] It is expected that the same is true in compound **3**, although the arrangement of the other ligands suggests this linkage may be almost linear.

The carbonyl and chloro ligands in complex **3** are normal, with parameters involving these ligands comparable to values previously reported.[1,12,15,19,20] The Ir(2)–C(2) distance is marginally longer than that of Ir(1)–C(1) (1.92 (1) vs 1.87 (1) Å) and is similar to the Ir–CO distance in another cationic hydride complex, $[Ir_2H(CO)_2(\mu\text{-}H)_2(DPM)_2][Cl]$,[12] in which the carbonyl is located opposite a hydrido ligand. This is taken as further support for the presence of a hydrido ligand opposite C(2), based on the known high trans influence that is exhibited by this ligand.[21]

Parameters within the metalated olefin groups are essentially the same as in the neutral dichloro species;[1] however, it should be noted that the carboxylate group involving C(6) is oriented with its methoxy substituent below the plane shown in Figure 2, while that involving C(12) has its methoxy group above the plane. This was

(18) Teller, R. G.; Bau, R. *Struct. Bonding (Berlin)* **1981**, *44*, 1.
(19) (a) Sutherland, B. R.; Cowie, M. *Inorg. Chem.* **1984**, *23*, 2324. (b) Sutherland, B. R.; Cowie, M. *Organometallics* **1985**, *4*, 1637.
(20) Kubiak, C. P.; Woodcock, C.; Eisenberg, R. *Inorg. Chem.* **1980**, *19*, 2733.
(21) Kaesz, H. D.; Saillant, R. B. *Chem. Rev.* **1972**, *72*, 231.

Table III. Distances (Å) in $[Ir_2(H)_2Cl(CH_3O_2CC{=}C(H)CO_2CH_3)_2(CO)_2(DPM)_2][BF_4]$

	Bonded		
Ir(1)-Cl	2.397 (3)	O(1)-C(1)	1.11 (1)
Ir(1)-P(1)	2.399 (3)	O(2)-C(2)	1.16 (1)
Ir(1)-P(3)	2.388 (3)	O(3)-C(5)	1.46 (2)
Ir(1)-C(1)	1.87 (1)	O(3)-C(6)	1.35 (2)
Ir(1)-C(7)	2.13 (1)	O(4)-C(6)	1.23 (2)
Ir(2)-P(2)	2.354 (3)	O(5)-C(9)	1.33 (2)
Ir(2)-P(4)	2.346 (3)	O(5)-C(10)	1.48 (2)
Ir(2)-C(2)	1.92 (1)	O(6)-C(9)	1.17 (2)
Ir(2)-C(13)	2.10 (1)	O(7)-C(11)	1.46 (2)
P(1)-C(3)	1.83 (1)	O(7)-C(12)	1.32 (2)
P(1)-C(21)	1.83 (1)	O(8)-C(12)	1.19 (2)
P(1)-C(31)	1.80 (1)	O(9)-C(15)	1.33 (1)
P(2)-C(3)	1.83 (1)	O(9)-C(16)	1.45 (1)
P(2)-C(41)	1.81 (1)	O(10)-C(15)	1.20 (1)
P(2)-C(51)	1.83 (1)	C(6)-C(7)	1.48 (2)
P(3)-C(4)	1.82 (1)	C(7)-C(8)	1.28 (2)
P(3)-C(61)	1.84 (1)	C(8)-C(9)	1.49 (2)
P(3)-C(71)	1.82 (1)	C(12)-C(13)	1.49 (2)
P(4)-C(4)	1.84 (1)	C(13)-C(14)	1.34 (2)
P(4)-C(81)	1.84 (1)	C(14)-C(15)	1.47 (2)
P(4)-C(91)	1.84 (1)		
	Nonbonded		
Ir(1)-Ir(2)	3.2895 (7)	O(1)-O(2)	3.07 (1)
P(1)-P(2)	3.151 (5)	C(1)-C(2)	3.11 (2)
P(3)-P(4)	3.143 (5)	O(1)-H(36)	2.26
Cl-H(8)	2.49	O(2)-H(42)	2.57

Table IV. Angles (deg) in $[Ir_2(H)_2Cl(CH_3O_2CC{=}C(H)CO_2CH_3)_2(CO)_2(DPM)_2][BF_4]$

Cl-Ir(1)-P(1)	82.7 (1)	Ir(2)-P(4)-C(4)	111.6 (4)
Cl-Ir(1)-P(3)	83.5 (1)	Ir(2)-P(4)-C(81)	112.9 (4)
Cl-Ir(1)C(1)	177.3 (4)	Ir(2)-P(4)-C(91)	118.8 (4)
Cl-Ir(1)-C(7)	90 (3)	C(4)-P(4)-C(81)	99.8 (5)
P(1)-Ir(1)-P(3)	165.4 (1)	C(4)-P(4)-C(91)	107.6 (5)
P(1)-Ir(1)-C(1)	96.3 (4)	C(81)-P(4)-C(91)	104.5 (5)
P(1)-Ir(1)-C(7)	94.3 (3)	C(5)-O(3)-C(6)	112 (1)
P(3)-Ir(1)-C(1)	97.1 (4)	C(9)-O(5)-C(10)	113 (1)
P(3)-Ir(1)-C(7)	90.9 (3)	C(11)-O(7)-C(12)	115 (1)
C(1)-Ir(1)-C(7)	91.9 (5)	C(15)-O(9)-C(16)	116 (1)
P(2)-Ir(2)-P(4)	155.9 (1)	Ir(1)-C(1)-O(1)	178 (1)
P(2)-Ir(2)-C(2)	104.6 (4)	Ir(2)-C(2)-O(2)	177 (1)
P(2)-Ir(2)-C(13)	90.1 (4)	P(1)-C(3)-P(2)	119.2 (6)
P(4)-Ir(2)-C(2)	99.2 (4)	P(3)-C(4)-P(4)	118.4 (5)
P(4)-Ir(2)-C(13)	91.8 (4)	O(3)-C(6)-O(4)	122 (2)
C(2)-Ir(2)-C(13)	94.1 (6)	O(3)-C(6)-C(7)	113 (1)
Ir(1)-P(1)-C(3)	108.0 (4)	O(4)-C(6)-C(7)	125 (2)
Ir(1)-P(1)-C(21)	113.4 (4)	Ir(1)-C(7)-C(6)	113 (1)
Ir(1)-P(1)-C(31)	121.8 (4)	Ir(1)-C(7)-C(8)	124 (1)
C(3)-P(1)-C(21)	103.6 (5)	C(6)-C(7)-O(8)	122 (1)
C(3)-P(1)-C(31)	106.1 (5)	C(7)-C(8)-C(9)	121 (1)
C(21)-P(1)-C(31)	102.6 (6)	O(5)-C(9)-O(6)	123 (2)
Ir(2)-P(2)-C(3)	110.3 (4)	O(5)-C(9)-C(8)	111 (1)
Ir(2)-P(2)-C(41)	123.9 (4)	O(6)-C(9)-C(8)	127 (2)
Ir(2)-P(2)-C(51)	110.0 (4)	O(7)-C(12)-O(8)	122 (2)
C(3)-P(2)-C(41)	104.4 (5)	O(7)-C(12)-C(13)	113 (1)
C(3)-P(2)-C(51)	100.1 (5)	O(8)-C(12)-C(13)	125 (2)
C(41)-P(2)-C(51)	105.5 (6)	Ir(2)-C(13)-C(12)	113 (1)
Ir(1)-P(3)-C(4)	108.8 (4)	Ir(2)-C(13)-C(14)	124 (1)
Ir(1)-P(3)-C(61)	121.9 (4)	C(12)-C(13)-C(14)	123 (1)
Ir(1)-P(3)-C(71)	114.1 (4)	C(13)-C(14)-C(15)	125 (1)
C(4)-P(3)-C(61)	103.2 (5)	O(9)-C(15)-O(10)	124 (1)
C(4)-P(3)-C(71)	104.1 (5)	O(9)-C(15)-C(14)	112 (1)
C(61)-P(3)-C(71)	103.2 (5)	O(10)-C(15)-C(14)	124 (1)

not the case in the neutral dichloro complex, which contained an approximate mirror plane perpendicular to the Ir–Ir bond. Such a difference is, no doubt, a consequence of the differing steric requirements in these compounds.

(b) Description of Chemistry. The reaction of $[Ir_2(H)_2(CO)_2(\mu\text{-}Cl)(DPM)_2][BF_4]$ (1) with 2 equiv of dimethyl acetylenedicarboxylate (DMA) in CH_2Cl_2 was previously found[1] to give a mixture of products, from which the neutral complex, $[Ir_2Cl_2(CH_3O_2CC{=}C(H)CO_2CH_3)_2(CO)_2(DPM)_2]$, was separated and structurally characterized. The X-ray structure determination of this neutral species offered support for the structure proposed for 1, due to the positions of the metalated olefin groups on the outsides of the complex, opposite the Ir–Ir bond. Since the source of an additional chloride ion was attributed to the CH_2Cl_2 solvent, it appeared that the mixture obtained in the reaction *did* contain the analogous cationic species but that it was sensitive to the solvent. It is now confirmed that the cationic doubly inserted species, $[Ir_2(CH_3O_2CC{=}C(H)CO_2CH_3)_2(CO)_2(\mu\text{-}Cl)(DPM)_2][BF_4]$ (2),

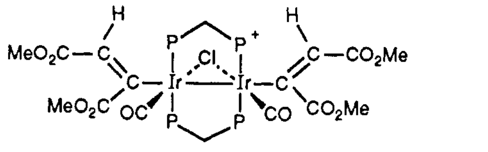

2

is exclusively obtained when the reaction is performed in either THF or acetone; the reaction occurs rapidly upon addition of DMA, causing a color change from yellow to orange–yellow. Addition of only 1 equiv of DMA to 1 merely yields 0.5 equiv of 2 and unreacted 1, as shown by $^{31}P\{^1H\}$ NMR spectroscopy. The symmetric nature of this species is evidenced by a singlet in the $^{31}P\{^1H\}$ NMR spectrum at δ −13.62 (see Experimental Section) and the ^1H NMR spectrum, which reveals only two carboxylate methyl resonances at δ 3.39 and 3.21 and one resonance at δ 3.52 for the two equivalent hydrogen atoms on the metalated olefin moieties. This contrasts the solution asymmetry found in the case of the neutral dichloro complex,[1] which was presumed to be due to steric crowding in the equatorial plane. The infrared spectrum of the isolated bright yellow solid displays two terminal carbonyl stretches at 2028 and 2013 cm^{-1}, bands due to the carboxylate groups, a C=C stretch for the metalated olefins, as well as a broad band at 1050 cm^{-1} characteristic of the BF_4^- counterion. Both carbonyl bands are at higher frequency than those of the dichloro species, as expected by the cationic nature of 2.

Clearly, the reaction of the dihydride complex, 1, with alkyne is rather facile, in spite of the coordinative saturation at both metals in 1. The mechanism proposed for the hydride rearrangement, yielding 1,[4] suggests a route to coordinative unsaturation at each metal center, allowing subsequent reaction with alkyne. As previously proposed, the bridging chloride ligand can swing into a terminal position on one metal, providing a site at the other metal for alkyne attack. Subsequent hydride migration to the coordinated alkyne, transfer of the chloride to the other metal, and a repeat of the above sequence at the second metal center must be very rapid since the reaction is immediate with no intermediate observed, even at low temperature. The similarity of the doubly inserted product (2) to the dihydride precursor (1) suggests that 2 should be capable of generating coordinative unsaturation at each metal by an analogous mechanism, and the observation that 1 reacts with H_2[1,4] suggests that compound 2 should likewise be capable of reaction with H_2. The resulting product would have adjacent hydrido and alkenyl ligands and should in principle be susceptible to subsequent reductive elimination of dimethyl maleate.

As anticipated, solutions of compound 2 react under an atmosphere of H_2 causing an immediate color change to very pale yellow, reminiscent of the pale coloration of the tetrahydrides formed when 1 is reacted with H_2.[1,4] The $^{31}P\{^1H\}$ NMR spectrum reveals a single unsymmetrical species, 3, having an AA′BB′ spin system with resonances at δ −7.90 (m) and −12.77 (m), and the ^{1}H NMR spectrum displays two broad hydride resonances at δ −8.76 and −19.37 at 22 °C, integrating as one proton each. However, at −40 °C the more downfield hydride resonance appears as a triplet ($^2J_{P-H}$ = 18.4 Hz) with coupling to two adjacent phosphorus nuclei, and by −80 °C the upfield hydride resonance is also somewhat better resolved into a multiplet. It is clear that the triplet represents a hydride that is terminally bound to one iridium center as evidenced by collapse of this resonance to a singlet upon selective decoupling of the ^{31}P resonance at δ −7.90. It is also evident that the hydride resonance at δ −19.37 corresponds to a hydride that bridges both metals, as observed in the partial collapse of this resonance during the selective decoupling experiment of each ^{31}P resonance. Although this resonance approaches the appearance of a pure triplet upon selective decoupling, the multiplicity is not very clear due to the poor resolution. Broad-band decoupling of both ^{31}P resonances from the ^{1}H NMR spectrum causes both hydride resonances to collapse to singlets. It is these NMR data as well as the observed positions of the other ligands found in the X-ray structure that suggest the locations of the two hydrido ligands as indicated in Figures 1 and 2.

The infrared spectrum of 3 displays two terminal carbonyl stretches (2051, 2016 cm^{-1}) and a weak band at 2135 cm^{-1} assigned to ν(Ir–H) by comparison of this spectrum to that of the analogous dideuteride, prepared by addition of D_2 to compound 2. Additional bands due to the carboxylate groups and the C=C stretch of the metalated olefins are also present. In the IR spectrum of the deuterated analogue (ν(CO), 2060, 2018 cm^{-1}) one of the two CO bands has shifted somewhat to higher frequency, consistent with this CO stretch having been coupled to the Ir–H stretch, supporting the location of a hydrido ligand opposite a carbonyl group.

The reaction of compound 2 with H_2 is in contrast to the failure of the neutral dichloro analogue, $[Ir_2Cl_2(CH_3O_2CC{=}C(H)CO_2CH_3)_2(CO)_2(DPM)_2]$, to react with H_2.[1] This reactivity difference is consistent with the mechanism noted earlier for generation of coordinative unsaturation in 2, which is not available to the dichloro analogue. As an interesting parallel, the cationic dihydride 1 also reacts with H_2, whereas the neutral analogue, $[Ir_2Cl_2(H)_2(CO)_2(DPM)_2]$, does not.[1]

The significance of compound 3 is appreciated when it is recognized that reports of characterized dihydroalkyl (-alkenyl) complexes are quite rare, even among the ever-increasing number of products of C–H activation.[22] Such species, which are often proposed as intermediates in hydrogenation, catalyzed by monohydride transition-metal complexes, are usually very unstable toward elimination of the hydrogenated product.[23] Furthermore, the structure of 3 is strong evidence that the chloride ligand can easily move to a terminal position, giving support to the mechanism by which hydride rearrangements occur and also by which coordinative unsaturation is generated to allow further reaction with alkynes or H_2.

Attempts to reductively eliminate the expected hydrogenated product, dimethyl maleate, from 3 have been unsuccessful. No reaction is observed upon addition of substitutive ligands such as CO or PMe_3 to compound 3. Neither is the olefin removed by heating solutions of 3 under N_2 purge, and instead prolonged relux in THF causes eventual H_2 loss. Such vigorous conditions required for H_2 loss suggests a high degree of stability, perhaps associated with exceptionally strong Ir–H bonds. This factor, as well as the presence of the electron-withdrawing carboxylate groups in the organic moiety resulting in strong Ir–C bonding,[24] appears to inhibit reductive elimination of the free olefin.

Although compound 1 reacts easily with DMA, no reaction is observed upon exposure of 1 to activated olefins such as dimethyl maleate and tetrafluoroethylene. These attempts were followed by monitoring the ^{31}P{^{1}H} NMR spectra over 24 h in the presence of excess olefin. In each case compound 1 was found to be the only phosphorus-containing species present in solution.

Due to the stability of complex 3 toward olefin loss, which is attributed, in part, to the stronger Ir–C bonds involving the activated alkenyl group, it was of interest to investigate the result of using unactivated alkynes for reaction with 1 and subsequent reaction with H_2. When phenylacetylene is reacted with 1, in the absence of H_2, the immediate appearance of small amounts of styrene and $[Ir_2(CO)_2(\mu\text{-}Cl)(DPM)_2][BF_4]$ as monitored by ^{1}H and ^{31}P{^{1}H} NMR spectra, respectively, indicates that some hydrogenation is apparently occurring in the absence of H_2 (vide infra). However in this reaction at least eight iridium–phosphine species are present, some of which also appear when the hydride-free cationic complex, $[Ir_2(CO)_2(\mu\text{-}Cl)(DPM)_2]^+$, is reacted with phenylacetylene. Although no species analogous to 2 could be identified in the reaction mixture, a species 4, which appears analogous

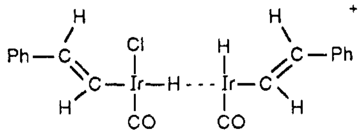

4

to 3, can be identified among the several species present when this mixture is reacted with H_2. At −40 °C compound 4 displays ^{31}P{^{1}H} resonances at δ −11.97 (m) and −18.21 (m) with an AA′BB′ pattern reminiscent of 3 and displays ^{1}H resonances due to two hydrides at δ −12.07 (br, 1 H) and −13.15 (t, $^2J_{P-H}$ = 16.5 Hz, 1 H), as well as methylene resonances of the DPM groups at δ 3.93 (m, 2 H) and 2.88 (m, 2 H). As was the case for 3, selective ^{31}P decoupling experiments on 4 identify the higher field resonance as resulting from a terminally bound hydride and the other as a bridging hydride. Irradiating the ^{31}P signal at δ −11.97 causes collapse of the high-field ^{1}H resonance to a singlet and changes the broad multiplet to a triplet ($^2J_{P-H}$ = 11.5 Hz), but irradiation of the ^{31}P signal at δ −18.21 affects only the low-field hydride resonance, changing it to a broad singlet. It appears that on the basis of the greater coupling to one set of phosphorus nuclei, in this case the bridging hydride ligand is associated more with the chloro-bound metal, with the weaker interaction being represented by the dashed line. Although at least eight species were present in solution, the phosphorus-decoupled ^{1}H NMR experiments clearly allow a correlation of the ^{31}P{^{1}H} and ^{1}H NMR resonances, although the resonances due to the metalated olefin moiety (—C(H)=C(H)Ph) could not be identified since they display no observable coupling to the

(22) A leading review containing many references is: Crabtree, R. *Chem. Rev.* **1985**, *85*, 245.

(23) James, B. R. In *Comprehensive Organometallic Chemistry*; Wilkinson, G., Stone, F. G. A., Abel, E. W., Eds.; Pergammon Press: Oxford, 1982; Vol. 8, p 285.

(24) (a) Lukehart, C. M. *Fundamental Transition Metal Organometallic Chemistry*; Wadsworth: Belmont CA, 1985; p 220. (b) Collman, J. P.; Hegedus, L. S.; Norton, J. R.; Finke, R. G. *Principles and Applications of Organotransition Metal Chemistry*; University Science Books: Mill Valley, CA, 1987; p 100.

Scheme I

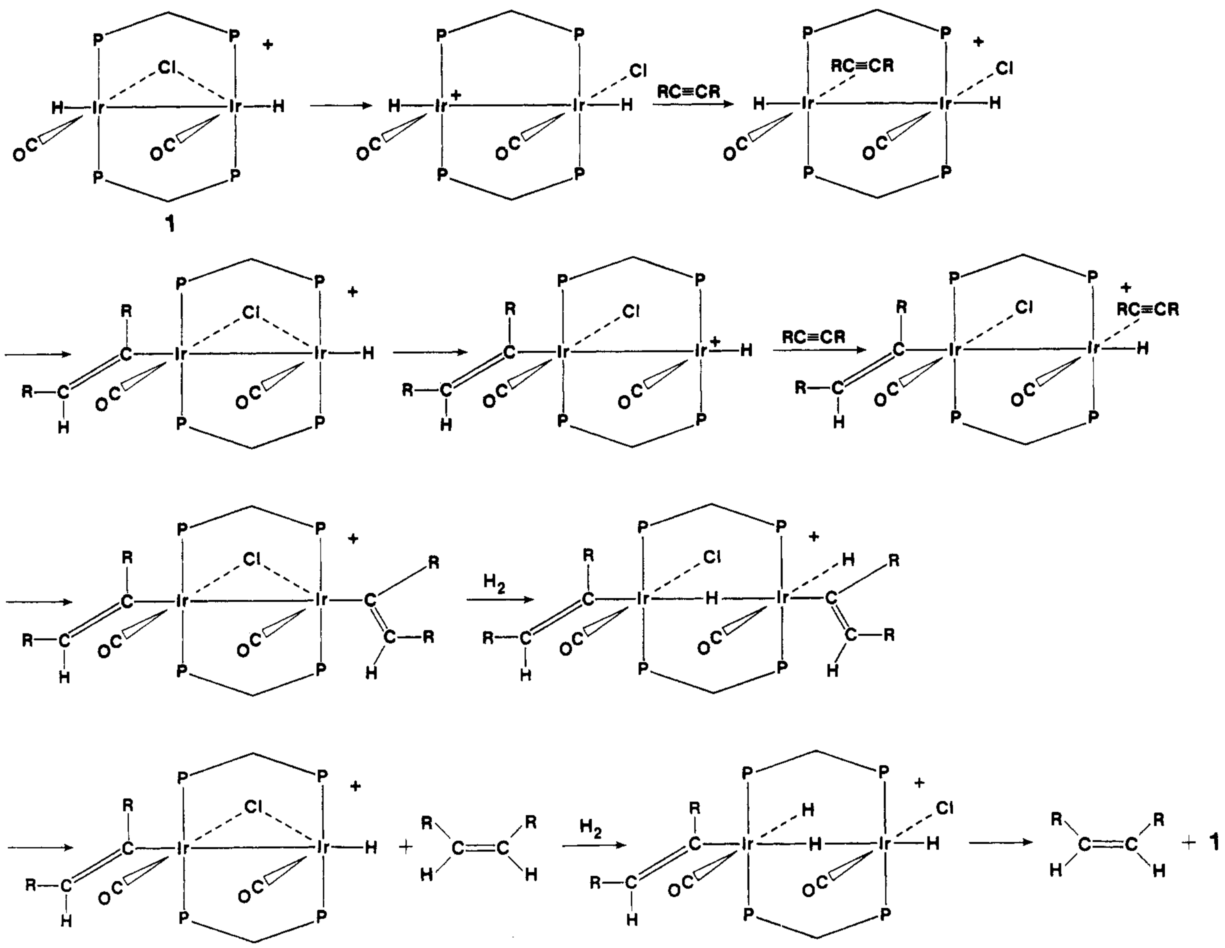

phosphorus nuclei. Similarly IR spectra of the mixture did not prove useful. With the above information compound 4 can be tentatively formulated as $[Ir_2(H)(Cl)(CO)_2(C(H){=}C(H)Ph)_2(\mu\text{-}H)(DPM)_2][BF_4]$, analogous to 3.

Within a few hours almost all species disappear, leaving only the known complexes $[Ir_2Cl(H)_4(CO)_2(DPM)_2][BF_4]$[1,4] and $[Ir_2(H)(CO)_2(\mu\text{-}H)_2(DPM)_2][BF_4]$.[12] The first species presumably results from reductive elimination of styrene (which was identified in the ^1H NMR spectra) and subsequent reaction of the $[Ir_2(CO)_2(\mu\text{-}Cl)(DPM)_2][BF_4]$ with H_2,[4] and the second species would seem to result from reductive elimination of HCl at some stage. The formation of this trihydride species, as well as the complex reaction mixture in the reactions involving phenylacetylene, clearly indicates that these reactions are more complex than with DMA. Nevertheless the observations of 4 suggests that one path for phenylacetylene hydrogenation by 1 is analogous to the reaction sequence involving DMA. We therefore propose Scheme I as one pathway by which alkynes can be hydrogenated by compound 1.

This mechanism is related to that previously proposed[4] for the hydride rearrangements leading to species 1 in that cleavage of one Ir–Cl bond yielding a 16-electron metal center is important. The steps leading to the doubly inserted chloro-bridged species have already been described earlier in this paper. Reaction of the doubly inserted product with H_2 yields the species analogous to 3, which although a stable species for 3 itself might be expected to reductively eliminate 1 equiv of olefin when nonactivated alkynes are used. A windshield-wiper motion of the chloro ligand is again suggested to generate a site for H_2 attack next to the other metalated olefin group, with subsequent elimination of the second olefin molecule to regenerate the dihydride 1.

As noted, the reaction of 1 with phenylacetylene yields small amounts of styrene even in the *absence* of H_2. It is found that reactions of 1 with 2-butyne and ethylene also lead to direct hydrogenation of the substrate. The reaction of excess 2-butyne with the dihydride, compound 1, causes an immediate color change from yellow to orange–yellow. Over 20 min the orange color intensifies, and after this time the $^{31}P\{^1H\}$ NMR spectrum reveals that the only phosphorus-containing species remaining is the A-frame complex, $[Ir_2(CO)_2(\mu\text{-}Cl)(DPM)_2][BF_4]$, which is identified by comparing the $^{31}P\{^1H\}$ NMR spectrum with that of an authentic sample. An infrared spectrum of the solution confirms that complete conversion to the A-frame complex has occurred. Analysis of a sample of the gas above the solution by gas chromatography reveals nearly equal concentrations of *cis*-2-butene and *trans*-2-butene as well as residual 2-butyne and a small amount of 1-butene. Note that H_2 is excluded from this reaction, and therefore direct butyne hydrogenation by 1 is occurring; clearly the route suggested by the DMA chemistry is not involved with this substrate. Similarly, the reaction of compound 1 with excess ethylene causes the solution to become orange in approximately the same time as the reaction with 2-butyne. Analysis of the gases above the solution by mass spectrometry verifies the presence of ethane. Removal of the ethylene/ethane atmosphere followed by recording of the infrared and $^{31}P\{^1H\}$ NMR spectra of the solution again reveals only the A-frame complex, $[Ir_2(CO)_2(\mu\text{-}Cl)(DPM)_2][BF_4]$.

Since the hydrido ligands in 1 are not mutually adjacent, an *intra*molecular mechanism for the hydrogenation of

2-butyne and ethylene appears unlikely. To provide support for an *inter*molecular reaction, a 1:1 mixture of $[Ir_2(H)_2(CO)_2(\mu\text{-}Cl)(DPM)_2][BF_4]$ (1) and its analogous dideuteride, $[Ir_2(D)_2(CO)_2(\mu\text{-}Cl)(DPM)_2][BF_4]$, was reacted with excess ethylene and the products analyzed by high-resolution mass spectrometry. The mass spectrum revealed that an approximate 1:2:1 ratio of C_2H_6, C_2H_5D, and $C_2H_4D_2$ had resulted, which is consistent with an intermolecular reaction. The same mechanism would appear reasonable for rationalizing the observation of *trans*-2-butene in reactions of 1 with 2-butyne; however, isomerization of an initially formed cis product by unreacted 1 could also explain its formation, along with the production of 1-butene.

The involvement of an intermolecular mechanism in the case of unactivated substrates is no doubt related to the iridium–carbon bond strengths in the metalated olefin intermediates. For 2-butyne and ethylene (and to some degree for phenylacetylene) these bonds are evidently weak and perhaps undergo homolytic bond cleavage such that the hydrogenation proceeds by a radical pathway. A radical mechanism has been supported in other hydrogenation reactions by the observation of chemically induced dynamic nuclear polarization (CIDNP) in the NMR experiment.[25] However, no such effects were evident in the ^1H NMR signal of the butenes when the reaction of 1 with 2-butyne was closely monitored by NMR.

Although the reaction of 1 with both 2-butyne and ethylene proceeds at attractive rates, 1 is not an effective catalyst for the hydrogenation of these substrates (at least under ambient conditions) due to very effective competition for the dihydride complex by H_2 to yield the coordinatively saturated tetrahydride isomers described previously.[4] Consequently, under conditions of high substrate concentration and low H_2 concentration needed to circumvent this problem, the catalysis is slow at best. Using substrate:H_2 mole ratios near 10:1, over solutions of the A-frame precursor of 1, caused no apparent H_2 uptake in the case of ethylene, and less than 1 turnover per hour was observed in the case of 2-butyne. Although an extensive study into this mechanism has not yet been undertaken, it is potentially important in catalytic hydrogenation by these systems and clearly should be investigated further. Studies of these reactions at elevated temperatures, where the tetrahydrides may be less likely to quench the reaction, would be of interest.

It was also of interest to compare the reaction of the related mixed-metal species $[RhIr(H)_2(CO)_2(\mu\text{-}Cl)(DPM)_2][BF_4]$ with DMA. This species is structurally rather different than the diiridium species, having both hydrido ligands bound primarily to one metal center (Ir) in the inside of the original A-frame "pocket".[4] This species does not react with DMA under ambient conditions and upon refluxing in CH_2Cl_2 yields $[RhIrCl(CO)_2(\mu\text{-}DMA)(DPM)_2][BF_4]$ as the major product (ca. 70% yield), identified by comparison of its spectral parameters with those of the species previously identified as either the perchlorate[26a] or the tetrafluoroborate[26b] salts. There is no evidence of any species resulting from insertion of DMA into the Ir–H bonds. This is possibly not surprising since for insertion to occur, attack by DMA in the crowded site between the metals would be necessary. It appears that location of the hydride ligands on the outside of the complex, as in 1, favors alkyne insertion since they are adjacent to the sites of coordinative unsaturation created by the "windshield-wiper" motion of the bridging chloride ligand.

The above mixed-metal dihydride also does not react with the activated alkenes, tetrafluoroethylene, and dimethyl maleate nor does it react with the unactivated substrates 2-butyne, phenylacetylene, and ethylene.

Conclusions

Although there are significant differences between the chemistry of the rhodium and iridium A-frame complexes, a study of the diiridium and mixed-metal "RhIr" complexes has provided useful insights into the catalysis by $[Rh_2(CO)_2(\mu\text{-}Cl)(DPM)_2]^+$. In particular, the crystal structure of 3 clearly establishes the ability of the bridging chloro ligand to open up a coordination site on one metal center by taking a terminal position on the other. This provides a great deal of support for the mechanism of hydride rearrangement described previously,[4] as well as the proposed mechanism for alkyne hydrogenation described in Scheme I, for which "windshield-wiper" movement of the anionic group is pivotal. The failure of the mixed RhIr complex, $[RhIr(H)_2(CO)_2(\mu\text{-}Cl)(DPM)_2][BF_4]$, to yield insertion products upon reaction with DMA suggests that the hydride rearrangement proposed[4] is an important step, minimizing the possibility of reductive elimination of H_2, which clearly competes with hydrogenation. It appears that the diiridium A-frame complex is an effective model for the dirhodium catalyst, with Scheme I representing a feasible mechanism by which alkynes could be hydrogenated by $[Rh_2(CO)_2(\mu\text{-}Cl)(DPM)_2]^+$. One should be cautious, however, in assigning this mechanism to the catalysis exclusively, as indicated by the intermolecular pathway shown here to be very facile for 2-butyne and ethylene hydrogenation, and by the obviously complex reactions occurring with phenylacetylene. Such pathways are, no doubt, available to the dirhodium system as well and perhaps through other hydride species in addition to the rearranged analogue of 1.

An important realization has come from these studies regarding metal–metal cooperativity in catalysis by these systems. Although the metals do cooperate by virtue of the coordinative unsaturation generated by the "windshield-wiper" mechanism, the actual hydrogenation occurs independently at each metal center. There is no evidence for interaction of the substrate with the adjacent metal during its insertion into the Ir–H bond; neither is a hydride on one metal ever observed to migrate to the unsaturated substrate on an adjacent metal. This does not say, however, that transmission of electronic effects of one metal to the other is not a factor. There is evidence that such electronic communication is easily transmitted through bridging ligands in iridium pyrazolate complexes.[27] Particularly of relevance to this work is the observation by Oro and co-workers[28] of the enhancement of catalysis by a second metal center in binuclear "RuRh" and "RuIr" complexes, which are more active than their mononuclear parent compounds in catalyzing the hydrogenation of cyclohexene. Further studies on these systems will hopefully determine whether such effects are involved and to what extent one metal can be tailored to enhance activity at the other.

Acknowledgment. We thank the Natural Sciences and Engineering Research Council of Canada (NSERC) and The University of Alberta for support of this work,

(25) Sweany, R. L.; Halpern, J. *J. Am. Chem. Soc.* **1977**, *99*, 8335.
(26) (a) Mague, J. T. *Organometallics* **1986**, *5*, 918. (b) Vaartstra, B. A. Ph.D. Thesis, University of Alberta.
(27) Bushnell, G. W.; Fjeldsted, D. O. K.; Stobart, S. K.; Zaworotko, M. J.; Knox, S. A. R.; Macpherson, K. A. *Organometallics* **1985**, *4*, 1107.
(28) Garcia, M. P.; Lopez, A. M.; Esteruelas, M. A.; Lahoz, F. J.; Oro, L. A. *J. Chem. Soc., Chem. Commun.* **1988**, 793.

NSERC for partial support of the diffractometer and structure determination package and for funding of the Perkin-Elmer gas chromatograph, and Dr. Gordon Nicol for assistance in interpreting mass spectral results.

Registry No. 1, 97690-07-8; 2, 126061-80-1; 3, 126061-82-3; 3·3THF, 126186-20-7; DMA, 762-42-5; $[Ir_2(D)_2Cl(CO)_2(DPM)_2][BF_4]$, 126061-84-5; $[Ir_2(CO)_2(\mu\text{-}Cl)(DPM)_2][BF_4]$, 90552-98-0; ethylene, 74-85-1; 2-butyne, 503-17-3; *cis*-2-butene, 590-18-1; *trans*-2-butene, 624-64-6.

Supplementary Material Available: Listings of anisotropic thermal parameters, additional bond lengths and angles, and hydrogen atom parameters (4 pages); listings of observed and calculated structure factors (29 pages). Ordering information is given on any current masthead page.

Crystal Structure and Solution-State NMR Spectra of 1,1′-(1,4,10-Trioxa-7,13-diazacyclopentadecane-7,13-diyldicarbonyl)ferrocene Hydrate

C. Dennis Hall,* Ian P. Danks, Stanley C. Nyburg, Adrian W. Parkins, and Nelson W. Sharpe

Department of Chemistry, King's College, University of London, Strand, London WC2R 2LS, U.K.

Received November 1, 1989

The crystal structure of the ferrocene-containing cryptand 1,1′-(1,4,10-trioxa-7,13-diazacyclopentadecane-7,13-diyldicarbonyl)ferrocene hydrate has been determined by X-ray crystallography. Crystals are orthorhombic, with a = 8.575 (6) Å, b = 13.512 (9) Å, c = 17.734 (11) Å, space group $P2_12_12_1$, and d(calcd, Z = 4) = 1.53 g cm^{-3}. The structure was solved from the Patterson function and refined by least squares; R_F = 0.056 (R_w = 0.058). The cyclopentadienyl rings are almost parallel, the dihedral angle between their least-squares planes being 3.2 (6)°, with an inter-ring separation of 3.28 (2) Å. The ferrocene rings are rotated from the eclipsed conformation by only ca. 0.3°. The orientation of the carbonyls is trans, with substitution at the cyclopentadienyl rings staggered by ca. 71.7°. The amide π-bonding systems exhibit only slight distortions from planarity. The proposed structure in solution as determined by 2-D homo- and heteronuclear NMR techniques is consistent with the X-ray structure.

Introduction

Ferrocene-containing macrocycles have attracted considerable attention in recent years, and a range of ferrocene-containing cryptands has been synthesized in this laboratory.[1,2] Their ability to complex metal cations offers the possibility for interaction between two metal centers. In particular, such compounds have yielded redox-active host molecules for selective recognition and binding of cations.[3,4] Ferrocene-containing macrocycles may be crownlike, for which several structures are known to date,[5–7] including one metal complex.[8] Alternatively, they may be cryptandlike, for which one previous structure has recently appeared,[9] together with that of a related compound,[10] both of which are symmetric. Knowledge of the structural types for such macromolecular hosts is important, since it affords information on the factors determining the structure-binding relationship with guest molecules or ions. This paper reports the first solid-state crystal structure for an asymmetric ferrocene-containing cryptand together with a detailed NMR analysis for the compound in solution.

Experimental Section

Synthesis. The title compound 1 was synthesized and purified by the general procedure outlined previously.[1] The product gave a satisfactory elemental analysis and relative molecular mass by mass spectroscopy. The crystal that proved suitable for X-ray studies was obtained by recrystallization from dichloromethane–ether.

Crystal Data, Structure Solutions, and Refinement. Crystal data for 1 were collected on a Picker four-circle diffractometer recently interfaced to an AT-TURBO 286 IBM-compatible microcomputer (full details to be published elsewhere) using Zr-filtered Mo Kα radiation and pulse height analysis. The dark orange crystal was mounted in a sealed Lindemann glass capillary, since the crystals appear to be unstable in air. It was almost totally obscured by epoxy resin such that its dimensions could not be measured. Crystal data: $C_{22}H_{28}N_2O_5Fe{\cdot}H_2O$, M_r = 474.33, a = 8.575 (6) Å, b = 13.512 (9) Å, c = 17.734 (11) Å, space group $P2_12_12_1$, d(calcd, Z = 4) = 1.53 g cm^{-3}. Intensity data were collected in the θ–2θ mode with a scan of 2° at 2° min^{-1}, with use of a modified version of a data collection program written by Grant and Gabe.[11] Only nonequivalent reflections were recorded to $2\theta_{max}$ = 50°, there being 1211 reflections out of 2072 having I(net) > $2.5\sigma[I(\text{net})]$. Structure analysis was carried out by using the NRCVAX package.[12]

Phasing, starting from the Patterson function, was uneventful. After full-matrix non-hydrogen anisotropic refinement most hydrogen positions could be found on the ΔF map. Except for those in the water molecule, they were given theoretical positions (C–H = 1.0 Å) and isotropic temperature factors equivalent to

(1) Hammond, P. J.; Bell, A. P.; Hall, C. D. *J. Chem. Soc., Perkin Trans. 1* **1983**, 707.
(2) Bell, A. P.; Hall, C. D. *J. Chem. Soc., Chem. Commun.* **1980**, 163.
(3) Hall, C. D.; Sharpe, N. W.; Danks, I. P.; Sang, Y. P. *J. Chem. Soc., Chem. Commun.* **1989**, 419.
(4) Andrews, M. P.; Blackburn, C.; McAleer, J. F.; Patel, V. D. *J. Chem. Soc., Chem. Commun.* **1987**, 1122.
(5) Bellon, P. L.; Demartin, F.; Scatturin, V.; Czech, B. *J. Organomet. Chem.* **1984**, *265*, 65.
(6) Bernal, I.; Raabe, E.; Reisner, G. M.; Bartsch, R. A.; Holwerda, R. A.; Czech, B. P.; Huang, Z. *Organometallics* **1988**, *7*, 247.
(7) Bernal, I.; Reisner, G. M.; Bartsch, R. A.; Holwerda, R. A.; Czech, B. P. *Organometallics* **1988**, *7*, 253.
(8) Akabori, S.; Habata, Y.; Sato, M. *Bull. Chem. Soc. Jpn.* **1984**, *57*, 68.
(9) Beer, P. D.; Bush, C. D.; Hamor, T. A. *J. Organomet. Chem.* **1988**, *339*, 133.
(10) Grossel, M. C.; Goldspink, M. R.; Knychala, J. P.; Cheetham, A. K.; Hriljac, J. A. *J. Organomet. Chem.* **1988**, *352*, C13–C16.
(11) Grant, D. F.; Gabe, E. J. *A Four-circle Diffractometer Control System*; National Research Council of Canada: Ottawa, Ontario, Canada, 1974.
(12) Gabe, E. J.; Lee, F. L.; Le Page, Y. *Crystallographic Computing 3: Data Collection, Proteins and Databases*; Sheldrick, G. M., Kruger, C., Goddard, R., Clarendon Press: Oxford, U.K., 1985; pp 167–174.

0276-7333/90/2309-1602$02.50/0